

Threshold and high-frequency behavior of dipole-bound anion photodetachment

V. E. Chernov and Boris A. Zon*

Voronezh State University, 394693, Russia, Voronezh, University Sq., 1

An explicit analytic description is given for dipole-bound anion (DBA) as an excess electron bound to the molecular neutral due to its dipole moment. The calculated DBA photodetachment cross-section displays $\propto \omega^{-2}$ behavior for large ω , in complete accordance with the experimental data [Bailey *et al.*, J. Chem. Phys **104**, 6976 (1996)]. At the threshold the photodetachment cross-section displays the Gailitis–Damburg oscillations.

PACS numbers: 33.80.Eh, 33.15.Ry

Considerable attention is paid presently to so-called dipole-bound anions (DBA), *i. e.* molecular negative ions in which the excess electron is bound to the molecular neutral (MN) due to its dipole moment [1]. Such structures play important role in various physical, chemical and biological processes [2].

As early as in 1947 Fermi and Teller [3] in their analysis of meson capture by hydrogen atoms noted that a fixed point dipole $d > 1.625$ D can bind an electron to an infinitely large number of bound states. A number of subsequent studies taking into account the finite dipole effects [4], presence of a short-range repulsive core potential [5], rotational excitation [6], polarization and quadrupolar interaction (see Ref. [7] and references therein) yield the minimum dipole moment 2–2.5 D required to form DBAs of common molecules [1, 8].

DBAs for experimental studies are created mainly by free electron attachment under high pressure nozzle expansion conditions [9, 10, 11, 12] and by charge transfer from Rydberg atoms [8, 13]. The created DBAs are investigated, *e. g.*, by photoelectron spectroscopy [9, 10, 11, 12, 13, 14].

Large-scale *ab initio* calculations (see, for instance, [12, 15, 16, 17] and references therein) of DBA structure studied the effects of correlation, orbital relaxation, dispersion and charge-transfer interaction. However, despite the increasing accuracy of such many-electron calculations, simplified one-electron local model potentials still have been proving their efficiency and suitability for large-scale computer simulations, as well as more analytical theories ([18] and references therein).

In this Letter we use simple model which considers DBA as an electron moving in a point dipole potential. The developed below simple analytic theory allows to explain some features of frequency-dependent DBA photodetachment. While the most of experimental photoelectron spectra are recorded at a constant photon frequency ω , the Reference [14] reports the photodetachment rate $\propto \omega^{-2}$. Such a behavior is different from the photodetachment cross-section $\propto \omega^{-7/2}$ in atoms [19] and $\propto \omega^{-3/2}$ in atomic negative ions [20], and can be easily explained using the proposed analytical technique. Our model also predicts oscillatory behavior of the cross-section near the threshold. Such oscillations were predicted for

electron scattered on hydrogen atom [21] and two-photon photodetachment of hydrogen anion with excitation of the residual atom [22]. The oscillations (as well as the linear Stark effect) are due to constant dipole moment of excited states of nonrelativistic hydrogen atom. Similar oscillations for electron scattering on polar molecules are discussed in [23].

We consider the MN to be a symmetric top whose rotational state is determined by its angular momentum j with the projection j_ζ onto the molecule-fixed ζ -axis directed along the MN dipole moment \mathbf{d} which is considered to be a point one. We also assume that MN remains in one of its vibrational states. The Hamiltonian of the excess electron moving in the field of the rotating MN is

$$\hat{H} = \hat{H}_{\text{rot}} + T_e + V(r, \cos \vartheta) = b_\xi \hat{j}^2 + (b_\xi - b_\zeta) \hat{j}_\zeta^2 + \frac{\hbar^2}{2m_e r^2} \frac{d}{dr} \left(r^2 \frac{d}{dr} \right) + \frac{\hbar^2 \mathbf{l}^2}{2m_e r^2} - \frac{\beta \cos \vartheta}{r^2}, \quad (1)$$

where \mathbf{l} is the electron orbital momentum, b_ξ and b_ζ are the MN rotational constants, \mathbf{r} is the electron radius-vector whose direction is determined by the spherical angles (ϑ, φ) in the molecule-fixed frame. Dimensionless dipole moment $\beta = 2m_e |e| d / \hbar^2 = 0.786 d(\text{D})$, e and m_e being the electron charge and mass.

The solution of Schrödinger equation with the Hamiltonian (1) can be found as a sum over the channels corresponding to different MN states:

$$\Psi = \sum_j R_j(r) \Phi_j, \quad (2)$$

where the angular functions Φ_j depend on ϑ, φ and on the MN coordinates. There are two limiting cases when the Schrödinger equation with the Hamiltonian (1) is separable. The first case, Born–Oppenheimer approximation (BOA), takes place when the MN rotation is slow compared to the electron motion. Quantitatively, the difference between the energy levels of the MN states with neighboring j values in BOA is small compared with the difference between the excess electron levels. The opposite limiting case, inverse Born–Oppenheimer approximation (IBOA) is fulfilled when the electron motion can be considered to be slow compared to the MN rotation. Thus in IBOA only one term remains

in (2) corresponding to the conserving MN angular momentum j ; such wavefunctions were used in rotationally adiabatic theory of rotational autodetachment of DBA [24].

The procedure of the separation of variables is given in detail in [25, 26] (BOA) and [27] (IBOA). In both cases the expression (2) is effectively reduced to a single-channel radial function multiplied by the appropriate angular function. The latter has more simple form in BOA case, so all the following results (which are not sensitive to the angular dependence of the electron wavefunction) will be formulated for BOA case.

The BOA angular functions $\mathcal{Z} \equiv \mathcal{Z}_{\lambda\eta}$ satisfy the equation

$$(-\hat{L}^2 + \beta \cos \vartheta) \mathcal{Z}_{\lambda\eta} = \eta \mathcal{Z}_{\lambda\eta} \quad (3)$$

and can be decomposed over the familiar spherical harmonics:

$$\mathcal{Z}_{\lambda\eta}(\vartheta, \varphi) = \sum_l a_{\eta l}^{(\lambda)} Y_{l\lambda}(\vartheta, \varphi).$$

Here the ζ -projection λ of the electron orbital momentum is conserved due the axial symmetry. This non-spheric symmetry results in l -mixing taken into account by the coefficients $a_{\eta l}^{(\lambda)}$. Together with these coefficients, $\mathcal{Z}_{\lambda\eta}$ depend on the eigenvalue η of the operator (3), and $\eta \rightarrow l(l+1)$, $l = 0, 1, \dots$ for $d \rightarrow 0$. This three-diagonal eigenvalue problem was studied in [25, 26] for application to Rydberg states in polar molecules. The functions \mathcal{Z} were used as early as in Debye's works on the Stark effect on polar molecules [28]. The same angular functions were used in analysis of the critical binding dipole moment in DBA [4] without studying the radial functions; for other references on usage of \mathcal{Z} functions see [25].

The radial functions satisfy

$$\frac{1}{r^2} \frac{d}{dr} \left(r^2 \frac{dR}{dr} \right) - \frac{\eta}{r^2} R + \frac{2m_e E}{\hbar^2} R = 0. \quad (4)$$

The solutions of the Eq. (4) for binding states ($E = -\hbar^2 \kappa^2 / (2m_e) < 0$) are McDonald functions (since they go to zero when $r \rightarrow \infty$):

$$R(r) = \frac{1}{\sqrt{r}} K_\rho(\kappa r), \quad \rho = \sqrt{\eta + 1/4}.$$

For real ρ these functions diverge at $r \rightarrow 0$:

$$K_\rho(\kappa r) \sim (\kappa r)^{-\rho}, \quad r \rightarrow 0, \quad (5)$$

so the existence (or absence) of binding electron states for $\eta > -1/4$ is determined by the behavior of the MN potential at small r .

If we consider only the binding due to the MN dipole moment, then these states arise for $\eta < -1/4$ when ρ is imaginary (it is easy to see that $\eta = -1/4$ corresponds to the above cited critical value $d = 1.625$ D). Applying a formula similar to (5) for imaginary ρ we see that the functions $R(r)$ oscillate for

$r \rightarrow 0$ according to (5) and $R(r) \sim \exp(-\kappa r)$ when $r \rightarrow \infty$. Assuming $s = i|\rho|$ the normalized radial wavefunctions are

$$R_{\kappa s}(r) = \left(\frac{2 \sinh \pi s}{\pi s} \right)^{1/2} \frac{\kappa}{\sqrt{r}} K_{is}(\kappa r), \\ s = \sqrt{|\eta| - 1/4}, \quad \eta < -1/4. \quad (6)$$

Oscillating behavior of wavefunctions (6) make them different significantly from the wavefunctions of an electron in δ -potential. Interestingly, the functions (6) satisfy all the necessary boundary conditions for all E . In other words, a *continuous spectrum of bound states* arises in the field of a point dipole with $\eta < -1/4$. In this sense it is an unique case in quantum mechanics (excluding more trivial cases, *e. g.*, quasicontinuous spectrum of bound states of an electron in a macroscopic potential box). The “falling to the center” (see the detailed comments in [29]) consists in that the energies of the bound states are not limited from below and the wavefunctions corresponding to different energies are not orthogonal.

Of course, this continuous spectrum of bound states is interesting only from the mathematical point of view, and connected with the fact that the Sturm–Liouville problem (4) has a singularity at $r = 0$. Physically, one should regularize the point dipole potential at small r . It can be achieved, for instance, by considering the MN as an extended dipole [4], taking into account some short-range repulsive core potential [5, 18]. We use the simplest regularization model of the nonpenetrating core. The boundary condition in this model reads as $R_{\kappa\rho}(r_0) = 0$ at some characteristic value of the MN radius r_0 . For $\kappa r_0 \ll 1$ we can use the formula like (5):

$$K_{is}(\kappa r) \simeq \frac{i}{2s} \left[\Gamma(1 - is) \left(\frac{\kappa r}{2} \right)^{is} - \Gamma(1 + is) \left(\frac{\kappa r}{2} \right)^{-is} \right] \\ = \frac{1}{s} \operatorname{Im} \left[\Gamma(1 + is) \left(\frac{\kappa r}{2} \right)^{-is} \right]$$

and obtain the electron energy spectrum:

$$\sin [s \ln(\kappa r_0/2) - \arg \Gamma(1 + is)] = 0, \\ E_{\lambda\eta n} = -\frac{2\hbar^2}{m_e r_0^2} \exp \left\{ -\frac{2\pi n}{s} + \frac{1}{s} \arg \Gamma(1 + is) \right\} \quad (7)$$

where $n = 1, 2, \dots$ is the “principal” quantum number and the dependence on η and λ is included through s . Note that a formula similar to (7) describes the spectrum of excited states of an electron in the finite-size dipole field [30]. The expression (7) should be applied carefully to low-excited DBA states; in the below calculation of photodetachment rate we do not use this formula.

For free electron states $E = \hbar^2 k^2 / (2m_e) > 0$ and the radial functions are expressed in terms of the Bessel functions whose order ρ may be either real or imaginary:

$$R_{k,s}(r) = \frac{1}{2\sqrt{r}} [J_{is}(kr) + J_{-is}(kr)], \quad \eta < -1/4,$$

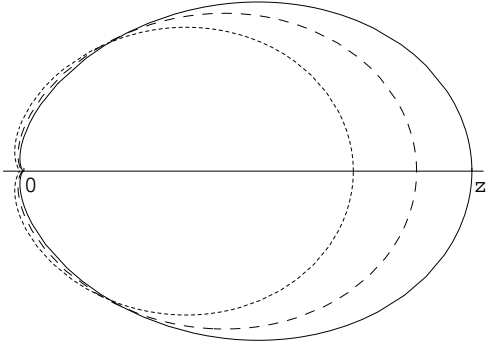


FIG. 1: Polar directional pattern of $|Z_{\lambda\eta}|^2$ for $\lambda = 0$ and $d = 3$ D ($\eta = -0.74$, dotted line), $d = 4$ D ($\eta = -1.18$, dashed line), $d = 5$ D ($\eta = -1.66$, solid line)

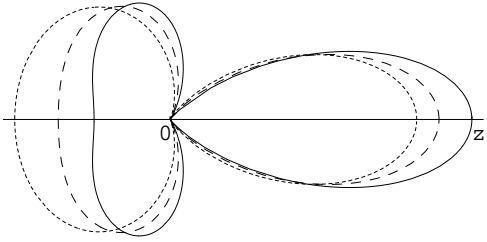


FIG. 2: Polar directional pattern of $|Z_{\lambda\eta}|^2$ for $\lambda = 1$ and $d = 3$ D ($\eta = 2.36$, dotted line), $d = 4$ D ($\eta = 2.5$, dashed line), $d = 5$ D ($\eta = 2.6$, solid line)

$$R_{k,\rho}(r) = \frac{1}{\sqrt{r}} J_\rho(kr), \quad \eta > -1/4. \quad (8)$$

Figure 1 shows the polar directional patterns of $|Z_{\lambda\eta}|^2$ for σ -states with $\eta < -1/4$ at different dipole moment values. Qualitatively, these patterns resemble those obtained by *ab initio* calculations (see, e. g., [12]). The same patterns for π -states with $\eta > -1/4$ are given in Fig. 2

The cross-section of the photodetachment in dipole approximation is

$$d\sigma_\varepsilon(\varkappa\lambda\eta; \omega) = \frac{\alpha m_e k \omega}{2\pi\hbar} \left| \langle \Psi_{\varkappa\lambda\eta} | r_\varepsilon | \Psi_{\mathbf{k}}^{(-)} \rangle \right|^2 d\Omega_{\mathbf{k}}.$$

Here $\alpha = e^2/\hbar c \simeq 1/137$, ω is the light field frequency, r_ε is projection of the electron coordinate onto the field polarization, $\Psi_{\varkappa\lambda\eta}$ is the wavefunction of the initial electron state. The wavefunction $\Psi_{\mathbf{k}}^{(-)}$ of the final state has the converging wave asymptotics. Its angular part can be constructed using the technique developed in [25] for BOA and in [27] for IBOA. The frequency dependence of $d\sigma_\varepsilon(\varkappa\lambda\eta; \omega)$ is determined only by the squared radial integral Q between the functions (6) and (8)

$$Q \propto \begin{cases} (k/\varkappa)^{\rho'} {}_2F_1(3/2 + \rho'/2 - is/2, 3/2 + \rho'/2 + is/2; 1 + \rho'; -k^2/\varkappa^2), & \eta' > -1/4 \\ (k/\varkappa)^{is'} {}_2F_1(3/2 + i(s-s')/2, 3/2 + i(s+s')/2; 1 + s'; -k^2/\varkappa^2) + (s \rightarrow s'), & \eta' > -1/4 \end{cases}, \quad (9)$$

where $k^2/\varkappa^2 = \hbar\omega/|E| - 1$ and the Eq. 7.7(31) in [31] to rewrite the radial integrals in terms of Gaussian hypergeometric functions. Depending on the relative energy of the MN rotation (*i. e.*, BOA or IBOA), the parameters s and ρ' (s') depend on the dipole moment as well as on λ , η and the MN rotational quantum numbers. The final ρ' (s') depends also on the radiation polarization ε .

The full cross section $\sigma_\varepsilon(\varkappa\lambda\eta; \omega)$ is the sum over the channels with different η' , similarly to the sum over the channels with different orbital momentum l in spherically symmetric case. The high-frequency limit $k^2/\varkappa^2 \rightarrow \infty$ can be obtained from (9) using the asymptotics of the hypergeometric functions given in [31], Eq. 2.1(17):

$$\sigma(\omega) \propto \omega^{-2}, \quad \hbar\omega \gg |E|. \quad (10)$$

The dependence (10) is common for both perpendicular and parallel ($\varepsilon = x$ or $\varepsilon = z$) polarization of the radiation as well as for all channels with $\eta > -1/4$ and $\eta < -1/4$. This dependence differs from photodetachment cross section in s -states of atomic negative ions ($\sigma(\omega) \propto \omega^{-3/2}$) but agrees with the experimental data [14] for DBA. The difference from

the zero-range potential model is due to the $\propto 1/\sqrt{r}$ behavior of the wavefunctions (8) in the small r domain that is different from the behavior $\propto 1/r$ of the wavefunctions in the zero-range potential. The $\propto \omega^{-2}$ behavior of $\sigma(\omega)$ holds also for the non-penetrating core model (7) provided the de Broglie wavelength of the excess electron is larger than the effective core radius: $k \sim \sqrt{2m_e\omega/\hbar} \lesssim 1/r_0$. Assuming $r_0 \sim 1 \text{ \AA}$, the photon frequencies $\sim 3 \text{ eV}$ used in Ref. [14] obey this condition. Actually, for much higher frequencies the ionization of the inner electronic shells becomes more probable than the detachment of the dipole-bound electron.

From the Eq. (9) one can also extract the behavior of the photodetachment cross-section at the threshold $k^2/\varkappa^2 \rightarrow 0$. Note that the factor $(k/\varkappa)^{\rho'}$ (9) suppresses the contribution of the $\eta' > -1/4$ channels at the threshold, and the main contribution is given by the $\eta' < -1/4$ channels. This fact has simple physical explanation. For $\eta' > -1/4$, the centrifugal repulsion of the electron exceeds its attraction by the dipole in the $r \simeq 0$ domain where the radial wavefunction is localized. Thus the radial wavefunction is small in $r \simeq 0$ domain because

the electron with $k \rightarrow 0$ cannot penetrate under the barrier. From the other hand, the barrier is absent for $\eta' < -1/4$ so that the radial function does not disappear in $r \simeq 0$ domain and the contribution of the corresponding channels remains finite at $k \rightarrow 0$. So we obtain

$$\sigma_{x,z}^{(\eta')}(\kappa\lambda\eta;\omega) \sim \cos^2[s'\ln(k/\kappa) + \psi_{ss'}], \quad (11)$$

where the phase $\psi_{ss'}$ does not depend on k . The result (11) differs significantly from the power Wigner law of the threshold photoeffect cross-section but it is similar to the threshold behavior of reactions involving the excited hydrogen atom [21, 22]. Note also that the dependence (11) cannot be obtained in Born approximation when the dipole influence on the free electron motion is neglected.

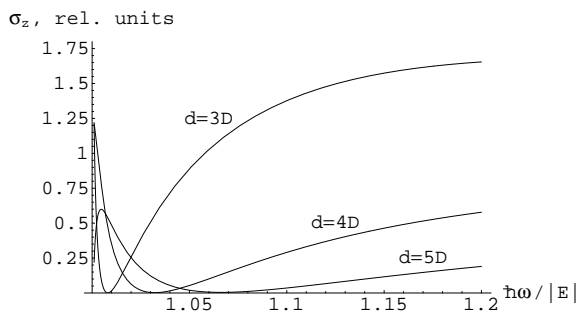


FIG. 3: Photodetachment cross-section in the near-threshold domain

Figure 3 shows the threshold behavior of the photodetachment cross-section σ_z when the radiation is polarized along the dipole direction. For the perpendicular polarization, the cross-section tends to zero since for $|\lambda| > 0$ one has $\eta > -1/4$ (the first value $\eta < -1/4$ arises for $\lambda = \pm 1$ at $d \simeq 9.646$ D). The cross-sections are given in relative units, their absolute values depend on the approximation (BOA or IBOA) used for the radial functions. It is seen that the cross-section is non-monotonic function of $\hbar\omega/|E|$ near the threshold.

We express our gratitude to R. Compton, pointed out the problem considered here, to D. Dorofeev, H. Helm I. Kiyan, and S. I. Marmo for helpful discussion. This work was partially supported by CRDF & Russian Ministry of Education (award VZ 010-0).

* Electronic address: zon@niif.vsu.ru

[1] R. N. Compton and N. I. Hammer, in *Advances in Gas-Phase Ion Chemistry*, ed. by N. Adams and I. Babcock (Elsevier Science, New York, 2001), Vol. 4, pp.257–291.

[2] C. von Sonntag, in *Physical and Chemical Mechanisms in Molecular Radiation Biology*, edited by W. A. Glass and M. N. Varma (Plenum, New York, 1991).

[3] E. Fermi and E. Teller, *Phys. Rev.* **72**, 399 (1947).

[4] J. M. Levy-Leblond, *Phys. Rev.* **153**, 1 (1967).

[5] O. H. Crawford, *Proc. R. Soc. (London)* **91**, 279 (1967).

[6] W. R. Garrett, *Chem. Phys. Lett.* **5**, 393 (1970); *Phys. Rev. A* **3**, 961 (1971); *J. Chem. Phys.* **77**, 3666 (1982).

[7] H. Abdoul-Carime and C. Desfrancois, *Eur. Phys. J. D* **2**, 149 (1998).

[8] C. Desfrancois, H. Abdoul-Carime, N. Khelifa, and J. P. Schermann, *Phys. Rev. Lett.* **73**, 2436 (1994).

[9] J. H. Hendricks, H. L. de Clercq, S. A. Lyapustina, and K. H. Bowen, *J. Chem. Phys.* **107**, 2962 (1997).

[10] S. Y. Han, J. H. Kim, J. K. Song, and S. K. Kim, *J. Chem. Phys.*, **109**, 9656 (1998).

[11] G. H. Lee, S. T. Arnold, J. G. Eaton, and K. H. Bowen, *Chem. Phys. Lett.* **321**, 333 (2000).

[12] M. Gutowski *et al.*, *Phys. Rev. Lett.*, **88**, 143001 (2002).

[13] R. N. Compton *et al.*, *J. Chem. Phys.* **105**, 3472 (1996).

[14] Ch. .G. Bailey, C. E. H. Dessent, M. A. Johnson, and K. H. Bowen, *J. Chem. Phys.* **104**, 6976 (1996).

[15] M. Gutowski, K. D. Jordan and P. Skurski, *J. Phys. Chem. A* **102**, 2624 (1998).

[16] K. A. Peterson and M. Gutowski, *J. Chem. Phys.*, **116**, 3297 (2002).

[17] A. Sawicka and P. Skurski, *Chem. Phys.* **282**, 327 (2002).

[18] F. Wang, and K. D. Jordan, *J. Chem. Phys.* **114**, 10717 (2001).

[19] M. Ya. Amusia, N. B. Avdonina, E. G. Drukarev, S. T. Manson, and R. H. Pratt, *Phys. Rev. Lett.* **85**, 4703 (2000).

[20] Yu. N. Demkov, V. N. Ostrovsky, *Zero-range potentials and their applications in atomic physics*, Plenum Press, New York (1988).

[21] M. Gailitis, and R. Damburg, *Zh. Eksp. Teor. Fiz.* **44**, 1644 (1963) [*Sov. Phys. JETP* **17**, 1107 (1963)].

[22] C. R. Liu, N. Y. Du, and A. F. Starace, *Phys. Rev. A* **43**, 5891 (1991).

[23] I. I. Fabrikant, *Zh. Eksp. Teor. Fiz.* **73**, 1317 (1977) [*Sov. Phys.-JETP* **46**, 693 (1977)].

[24] D. C. Clary, *J. Phys. Chem.* **92**, 3173 (1988).

[25] B. A. Zon, *Zh. Eksp. Teor. Fiz.* **102**, 36 (1992) [*Sov. Phys. JETP* **75**, 19 (1992)].

[26] J. K. G. Watson, *Mol. Phys.* **81**, 227 (1994).

[27] B. A. Zon, *Phys. Lett. A* **203**, 373 (1995); *Laser Phys.* **7**, 806 (1997).

[28] P. Debye, *“Polar Molecules”*, New York: Chemical Catalog Co., 1929.

[29] L. D. Landau and E. M. Lifshitz, *“Quantum Mechanics (Non-relativistic Theory)”*, Pergamon, Oxford, 1977.

[30] G. F. Drukarev, *Electron collisions with atoms and molecules*, Moscow, Nauka (1978, in Russian).

[31] Higher Transcendental Functions, eds. H. Bateman and A. Erdelyi, McGraw-Hill (1953).